[4] D. D. C. Bradley, R. H. Friend, H. Lindenberger, S. Roth. *Polymer* **1986**, *27*, 1709.
[5] M. Fahlman, J. Rasmusson, K. Kaeriyama, D. T. Clark, G. Beamson, W. R. Salaneck, *Synth. Met.* **1994**, *66*, 123.
[6] V. Massardier, V. B. Cajipe, T. P. Nguyen, V. H. Tran, *Synth. Met.* **1995**, *75*, 169.
[7] V. Cimrová, M. Remmers, D. Neher, G. Wegner, *Adv. Mater.* **1996**, *8*, 146.
[8] S. Hotta, K. Waragai, *J. Mater. Chem.* **1991**, *1*, 835.
[9] F. Garnier, A. Yassar, R. Hajlaoui, G. Horowitz, F. Deloffre, B. Servet, S.Ries, P. Alnot, *J. Am. Chem. Soc.* **1993**, *115*, 8716.
[10] B. Servet, S. Ries, M. Trotel, P. Alnot, G. Horowitz, F. Garnier, *Adv. Mater.* **1993**, *5*, 461.
[11] B. Servet, G. Horowitz, S. Ries, O. Lagorsse, P. Alnot, A. Yassar, F. Deloffre, P. Srivastava, R. Hajlaoui, P. Lang, F. Garnier, *Chem. Mater.* **1994**, *6*, 1809.
[12] J. C. Wittmann, P. Smith, *Nature* **1991**, *352*, 414.
[13] R. E. Gill, A. Meetsma, G. Hadziioannou, *Adv. Mater.* **1996**, *8*, 212.
[14] H. E. Katz, S. F. Bent, W. F. Wilson, M. L. Schilling, S. B. Ungashe, *J. Am. Chem. Soc.* **1994**, *116*, 6631.
[15] S. Meyer, P. Smith, J. C. Wittmann, *J. Appl. Phys.* **1995**, *77*, 5655.

Electrodeposition of Quantum-Confined Metal/Semiconductor Nanocomposites**

By *Jay A. Switzer,* Chen-Jen Hung, Eric W. Bohannan, Mark G. Shumsky, Teresa D. Golden,* and *David C. Van Aken*

Quantum confinement of carriers in nanometer-scale materials leads to size-dependent optical and electrical properties that are intermediate between those of molecules and those of extended network solids. The quest in this area of research is to engineer a normally intrinsic property such as a semiconductor bandgap by simply changing the size of the material. Semiconductors in this size regime can also show enhanced carrier mobility, nonlinear optical properties, and quantized charge transport. Examples of quantum-confined materials include superlattices,[1,2] quantum dots,[3–6] and surface-confined systems such as quantum corrals.[7] Work on chemically produced nanometer-scale materials has mostly focused on toxic, heavy-metal chalcogenides such as CdS and CdSe.[3,5,6] Since it is difficult to make actual devices out of individual quantum dots, these materials have not been technologically exploited. Here we show that composite films of copper and cuprous oxide can be electrochemically assembled at room temperature from aqueous solution precursors with crystallite radii in the 5–10 nm range. Although the confinement dimensions are in the nanometer range, the strongly adherent and conformal films can be deposited over areas of several square centimeters, and they should be device-friendly. The phase composition and color of the nanophase architectures can be tuned by simply varying the applied current density.

Cuprous oxide, Cu_2O, is a relatively non-toxic, p-type semiconductor with a bandgap of approximately 2 eV. Interest in the semiconducting properties of the material began as early as 1926, when Grondahl produced the Cu/Cu_2O rectifier.[8] Cuprous oxide is also a textbook example of a Wannier–Mott excitonic solid.[9] An exciton is a bound electron–hole pair that is produced at photon energies slightly less than the semiconductor bandgap energy. A Wannier–Mott exciton is weakly bound and can have an exciton diameter that extends over several unit cells, whereas a Frenkel exciton is tightly bound and is usually localized on the anion of an ionic solid. Up to 10 hydrogen-like exciton lines can be seen in the absorption spectrum of Cu_2O at low temperatures.[10–12] Unbound excitons in Cu_2O have a binding energy of 150 meV, and a radius of 0.7 nm. For comparison, the exciton radii in CdS and CdSe are 2.7 and 5.4 nm, respectively.

The physics community is presently very excited about the excitonic properties of Cu_2O, since there is evidence that Bose–Einstein condensation of excitons can occur in the material.[13] Since the effective mass of the excitons is very small (close to that of a free electron) the de Broglie wavelength is large, and condensation can be observed at relatively high temperatures. Because excitons, like photons, are bosons, they can be made to propagate though a solid coherently.[14] There is a very important potential application of this phenomenon. It may be possible to transmit light though an aperture or fiber with nanometer dimensions without loss to diffraction. The photon can be converted into an exciton, which stores the energy in the electronic state with short wavelength while passing though the aperture, and the exciton can then convert back into a photon on the other side.[15] Studies of Bose–Einstein condensation of excitons in Cu_2O have all been on single-crystal samples. There have been no studies to date of this effect on nanophase Cu_2O.

Although most research on quantum-confined materials has emphasized the growth of architectures with dimensions as small as possible, Brus has suggested that the weak confinement limit (that is, the quantum dot radius greater than four times the exciton radius) is desirable for electro-optic and all-optical nonlinear optical applications.[4] In the weak confinement limit, the optical absorption spectrum is expected to blue-shift slightly due to the interaction of two or more excitons in the same particle. The oscillator strength is greatly enhanced (the so-called "giant" oscillator strength) in the weak confinement limit due to the co-

[*] Prof. J. A. Switzer, C.-J. Hung, E. W. Bohannan, Dr. M. G. Shumsky, Dr. T. D. Golden
Department of Chemistry and
Graduate Center for Materials Research
University of Missouri – Rolla
Rolla, MO 65409-1170 (USA)
Prof. D. C. Van Aken
Department of Metallurgical Engineering
University of Missouri – Rolla
Rolla, MO 65409-1170 (USA)

[**] This work was supported by National Science Foundation grant DMR-9202872, Office of Naval Research grants N00014-96-1-0984 and N00014-94-1-0917, and the University of Missouri Research Board.

© VCH Verlagsgesellschaft mbH, D-69469 Weinheim, 1997
0935-9648/97/0403-0334 $ 10.00+.25/0

ADVANCED MATERIALS

herent excitation of the excitons in the quantum box. If the particles are too small, and they reach the strong confinement limit (that is, the particle radius is much less than the exciton radius), the electron and hole are individually confined, with little electron–hole correlation.

Hence, it should be possible to make quantum dots of Cu_2O if the crystallite size or confinement dimensions can be reduced to the weak confinement limit. Kellersohn et al. have produced Cu_2O crystallites with a 4.5 nm radius by thermally oxidizing nanocrystalline copper.[16] The optical absorption spectrum of the nanocrystalline Cu_2O was blue-shifted 0.6 eV relative to that of the bulk semiconductor.

Our approach to the nanometer-scale regime is electrodeposition. Martin has electrodeposited nanometer-scale materials into the pores of nanophase membrane templates.[17] Rubinstein, Hodes, and co-workers have produced epitaxially-oriented CdSe quantum dots with diameters of about 5 nm by electrodepositing the nanocrystals onto evaporated gold substrates.[18] The size of the quantum dots is believed to be controlled by the strain that is induced by the CdSe/Au lattice mismatch. We have previously shown that both compositional[19–22] and defect-chemistry[23] superlattices of metal oxide semiconductors can be grown by pulsing the applied potential or current during deposition. The materials in our previous work were highly-conducting degenerate semiconductors.[24] For example, in the case of the electrodeposited defect-chemistry superlattices based on thallium(III) oxide it was shown that material with cation interstitials was deposited at low overpotential and material with oxygen vacancies was deposited at high overpotential.[23] Superlattices with layers as thin as 3 nm were grown by pulsing the applied potential during deposition.

A fascinating aspect of the present system is that the potential oscillates *spontaneously* if a constant current density is applied to the cell. The Cu/Cu_2O nanocomposites are only produced when oscillations of the potential are observed. An example of these potential oscillations is seen in Figure 1 for deposition at an applied cathodic current density of 0.5 mA/cm^2 from a solution of 0.6 M Cu^{II}, 3 M lactate ion, and a pH of 9.[25,26] Potential oscillations are observed when the current density is greater than about 0.1 mA/cm^2. At current densities below that value, highly oriented films of red Cu_2O are deposited, and at higher current densities nanocomposites are deposited, with a color and phase composition which depend on the applied current density. The color of the films varies from red at a current density of 0.05 mA/cm^2, to green at a current density of 0.5 mA/cm^2, to metallic gold at a current density of 2.5 mA/cm^2. We have deposited films of the composites onto stainless steel, indium tin oxide, copper, and platinum substrates.

Potential and current oscillations are quite common in electrodeposition.[27–29] The oscillations are often caused by the adsorption and dissolution of an insoluble layer. Electrochemical oscillations that are particularly relevant to the present work are those observed during the anodic dissolution of copper metal in solutions containing acetate ion. Dewald et al. attribute these oscillations to the deposition and dissolution of passivating films of basic copper acetate.[29] Since we do not observe oscillations using a solution at pH 12, we believe that the oscillations in the pH 9 solution may be caused by the precipitation of a neutral Cu^{II} lactate complex produced by the reduced local pH at the electrode surface during oxide formation at higher current densities. The surface layer would subsequently be reduced to copper metal.

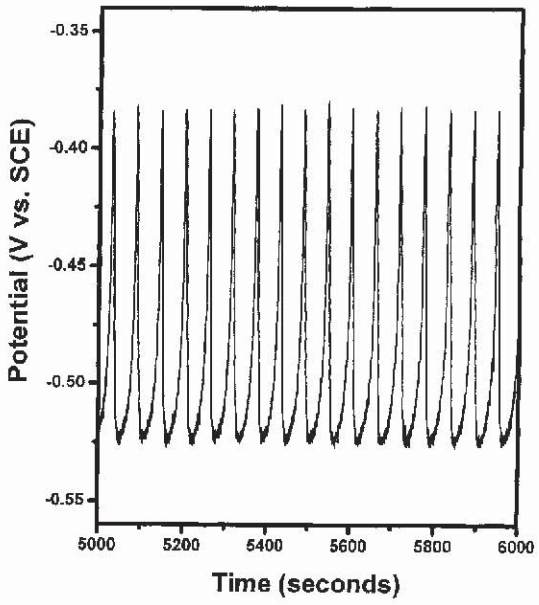


Fig. 1. Oscillations of the electrode potential observed during deposition of a Cu/Cu_2O nanocomposite at an applied cathodic current density of 0.5 mA/cm^2. The deposition solution is 0.6 M Cu^{II}, 3 M lactate ion, and a pH of 9.

Figure 2 shows X-ray diffraction (XRD) patterns for 10 μm thick films deposited at current densities of 0.05 (top) and 0.5 mA/cm^2 (bottom). The film grown at 0.05 mA/cm^2 is Cu_2O with a strong [100] orientation. Notice that only the [200] and [400] reflections are observed, and that the peaks are relatively narrow. No Cu peaks are observed in the XRD pattern of a pulverized sample of this material. In contrast, the XRD pattern of the film grown at 0.5 mA/cm^2 shows a random orientation of both Cu and Cu_2O, and peaks that are broadened due to the small crystallite size. Rietveld analysis[30] of the XRD pattern shows that the sample is 50 mol-% Cu and 50 mol-% Cu_2O. Using the Scherrer equation,[31] the crystallite radii of Cu and Cu_2O are estimated to be 6 and 12 nm, respectively. The crystallite radii were measured from the [200] reflection of Cu and the [111] reflection of Cu_2O. For the thin films used for optical studies, the crystallite radii were determined by transmission electron microscopy.

The phase composition can be controlled by varying the applied cathodic current density used to deposit the films. At current densities below 0.1 mA/cm^2 the films are 100 %

 © VCH Verlagsgesellschaft mbH, D-69469 Weinheim, 1997 0935-9648/97/0403-0335 $ 10.00+.25/0

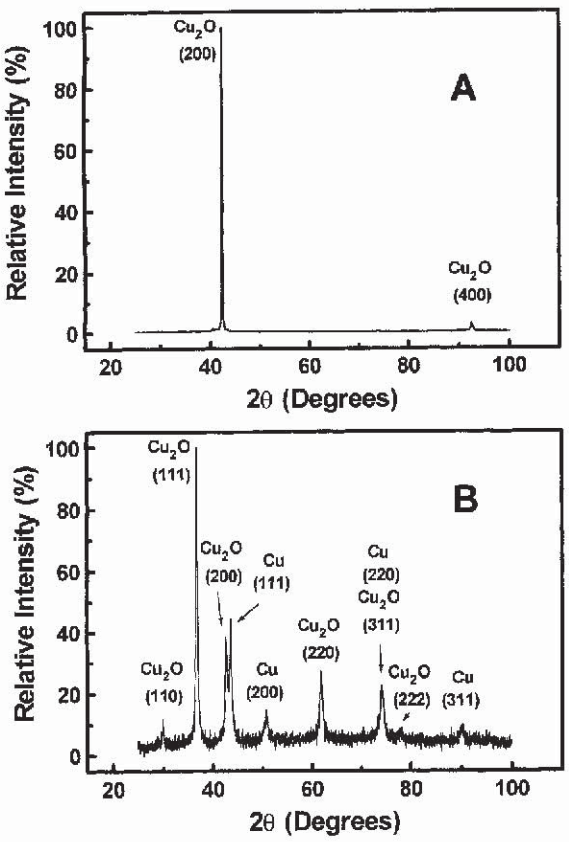


Fig. 2. Comparison of the X-ray diffraction (XRD) patterns of a pure Cu_2O film (A) deposited at 0.05 mA/cm^2 and a Cu/Cu_2O nanocomposite film (B) deposited at 0.5 mA/cm^2. The Cu_2O film has a strong [100] orientation and large crystallite sizes, while the Cu/Cu_2O film is randomly oriented. The crystallite radii of Cu and Cu_2O are estimated to be 6 and 12 nm, respectively. The phase composition of the nanocomposite is 50 mol-% Cu and 50 mol-% Cu_2O. Films were deposited onto 1.5 cm^2 polycrystalline Pt substrates.

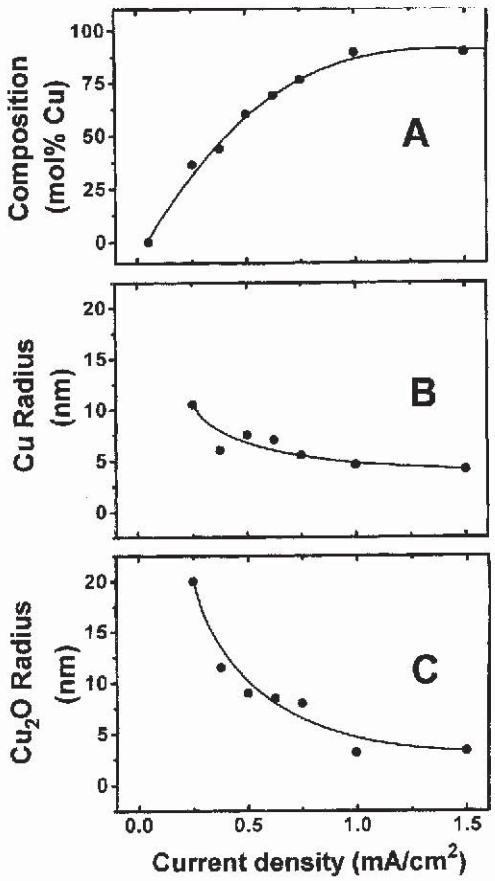


Fig. 3. Phase composition (A), Cu particle radii (B), and Cu_2O particle radii (C) for nanocomposites as a function of the applied current density. Measurements were made by XRD on 10 μm thick films, which were deposited onto 1.5 cm^2 polycrystalline Pt substrates.

Cu_2O according to XRD. As the current density is increased, the Cu content increases from 37 mol-% at 0.25 mA/cm^2 to 98 mol-% at 2.5 mA/cm^2. This is a key advantage of the electrochemical method. A desired phase composition can be deposited at a constant current using a potentiostat/galvanostat or a simple constant-current power supply. The crystallite radii for both Cu and Cu_2O decrease as the current density is increased. The phase composition and crystallite radii for Cu and Cu_2O as a function of deposition current density are presented in Figure 3. At applied current densities greater than 0.5 mA/cm^2, the crystallite radii of both Cu and Cu_2O are less than 10 nm. Another advantage of this simple and inexpensive deposition method is that the nanocrystalline Cu and Cu_2O are directly co-deposited at room temperature as strongly adhering films. No heat-treatment or consolidation step is necessary.

The potential oscillations observed during the deposition of all of the composites would suggest that the materials are modulated. For example, the period in the potential oscillations in Figure 1 of 58 s would correspond to a modulation wavelength of approximately 20 nm. Microstructural analysis by cross-sectional transmission electron microscopy (TEM) is presently in progress to determine if these materials are multilayers or granular nanocomposites. Copper has a face-centered cubic structure with space group Fm3m and a lattice parameter of 0.3615 nm, whereas Cu_2O has a primitive cubic structure with space group $Pn\bar{3}$ and a lattice parameter of 0.4266 nm.[26] The 15 % mismatch between the lattice parameters of the two materials may lead to relaxation of coherency and island formation. It may, however, be possible to grow a layered structure if the thickness of the layers is maintained below a critical value.

The optical properties of the nanocomposites are a function of both the nanophase Cu_2O and Cu in the films. Specular reflectance spectra of the composites are shown in Figure 4, along with the spectra of both thin film and bulk Cu, and a thick film of Cu_2O with large grains. The Cu and composite films were all grown to a charge density of 0.1613 C/cm^2 (nominal thickness of 0.1–0.2 μm). The reflectance in the 0.5–2.2 eV range of the spectrum is dominated by the Cu in the films. As the Cu content increases, the reflectance increases. The reflectance due to Cu drops off sharply at 2.1–2.2 eV, which we attribute to the plasma resonance for Cu.

© VCH Verlagsgesellschaft mbH, D-69469 Weinheim, 1997
0935-9648/97/0403-0336 $ 10.00+.25/0

ADVANCED MATERIALS

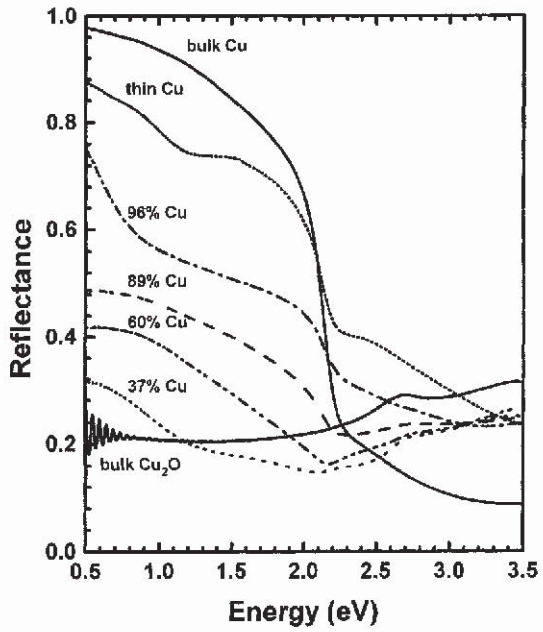


Fig. 4. Specular reflectance spectra of electrodeposited Cu/Cu_2O nanocomposites with various phase compositions, thin and bulk Cu metal, and a film of Cu_2O with micrometer-sized crystallites (bulk Cu_2O).

The absorption spectra for the nanocomposites and thin Cu and thick Cu_2O films are shown in Figure 5. Cu absorbs strongly in the near IR, and the absorption goes through a minimum at 2.2 eV. It is interesting that the plasmon resonance for Cu in the composites is located at an energy slightly below the onset of the Cu_2O absorption. The plasmon resonance of the composite containing 96 % Cu is at 1.85 eV (669 nm), compared with 1.27 eV (973 nm) for the thin film of pure Cu. Absorption due to the Cu_2O in the films is low in the near IR, but rises sharply in the band-to-band region. The absorption rises at about 2.0–2.1 eV for bulk Cu_2O, and is blue-shifted to about 2.5 eV for the composites.

Plots of the optical absorption coefficient, α, versus energy of large-grained Cu_2O deposited at 0.05 mA/cm^2 and a composite deposited at 0.5 mA/cm^2 are shown at the top of Figure 6. The crystallites in the pure Cu_2O film were larger than 1 μm, whereas the radius of the Cu_2O crystallites in the composite was estimated from XRD to be 10 nm, and by TEM to be 8±2 nm. Crystallites of Cu_2O in the composite films used for optical studies were smaller that those shown in Figure 3, since the films for the optical studies were much thinner (typically 0.1–0.2 μm) than the films used for phase analysis (10 μm). The absorption of Cu in the composite films precludes the use of thick films for optical studies. The absorption edges for nanocrystalline and bulk Cu_2O were determined at the bottom of Figure 6 from a plot of $(\alpha E)^2$ versus E.[24,26] The absorption edge for bulk Cu_2O is 2.1 eV, while the absorption edge for the 8 nm radius crystallites in the nanocomposite is 2.5 eV.

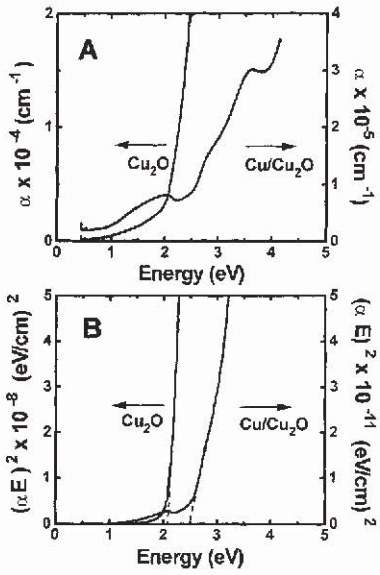


Fig. 6. Optical absorption spectra (A) and plots of $(\alpha E)^2$ versus E (B) to determine the energy of the direct optical absorption edges for bulk Cu_2O and Cu/Cu_2O deposited at 0.5 mA/cm^2. The absorption edge for the bulk Cu_2O is 2.1 eV, whereas the absorption edge for the 8 nm radius crystallites in the nanocomposite is blue-shifted to 2.5 eV. We attribute the absorption at about 2 eV in the composite to a Cu surface plasmon resonance.

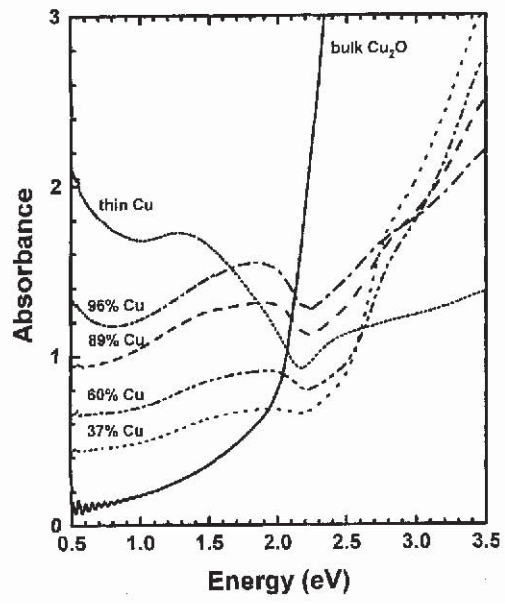


Fig. 5. Plots of absorbance versus energy for electrodeposited Cu_2O nanocomposites (same films as Fig. 4), thin Cu metal, and a film of Cu_2O with micrometer-sized crystallites (bulk Cu_2O).

The blue-shift of 400 meV, 20-fold enhancement in optical absorption, and development of discrete features in the absorption spectrum of the nanocomposite are all consistent with quantum confinement of the 0.7 nm excitons in the 8 nm crystallites. The observed shift, though, of 400 meV is much larger than the 2 meV shift that would be expected for a ratio of the crystallite radius to exciton radius of 11.[32] This anomalously large shift may be caused by a confinement dimension which is smaller than the crys-

 © VCH Verlagsgesellschaft mbH, D-69469 Weinheim, 1997 0935-9648/97/0403-0337 $ 10.00+.25/0

tallite size (due to strain or Schottky barrier formation), or to a condensation of the excitons to a droplet with an effective radius which is larger than the individual exciton radius. A study of the absorption and emission spectra of the composites as a function of crystallite size, temperature, and photon flux should help to unravel the cause of this unusually large blue-shift. We are also measuring the electrical properties of these composites. The materials should function like electron percolation solids. Copper metal has a resistivity in the μΩ cm range, whereas the resistivity of cuprous oxide is in the MΩ cm range. It will be interesting to determine whether the electrical properties are dominated by the large area of Schottky-like barriers which should form at the Cu/Cu_2O interfaces.[8]

In summary, we have shown that it is possible to electrodeposit nanocomposite films of Cu and Cu_2O at room temperature from an alkaline aqueous solution of Cu^{II} lactate. The phase composition varies from pure Cu_2O at cathodic current densities below 0.1 mA/cm^2 to 98 mol-% Cu at 2.5 mA/cm^2. The electrode potential oscillates spontaneously during constant-current deposition of the composites. The Cu_2O crystallites in the nanocomposite have the optical properties of quantum dots. The optical absorption edge blue-shifts from 2.1 eV for the bulk material to 2.5 eV for the 8 nm radius crystallites, discrete features develop in the spectrum, and there is an approximately 20-fold increase in the absorption coefficients for the quantum-confined semiconductor.

Experimental

All solutions were made from reagent-grade chemicals dissolved in HPLC grade water from Aldrich. To prepare the deposition solution, 90 g of copper sulfate was added to 150 mL of 85 % lactic acid with stirring. Over a period of a few minutes, 450 mL of 5 M NaOH was added in 50–100 mL increments. The solution was stirred overnight, and then the pH was adjusted to 9.0 with the addition of 10–20 mL of 5 M NaOH. Deposition currents were controlled with an EG&G Model 273A potentiostat/galvanostat, and the potential oscillations were recorded on a Nicolet Pro 10 oscilloscope. A constant temperature of 30 °C was maintained during deposition.

The specular reflectance and absorption spectra were run on a CARY 5 UV-Vis-NIR spectrophotometer. For optical measurements, the films were first grown onto 430 polycrystalline stainless steel electrodes that were potted in epoxy so that only the front surface was exposed to the solution. The films were then peeled off onto microscope slides using Super Glue from 3M. The microscope slides and glue do not absorb appreciable light at energies below 3.5 eV. The absorption coefficient, α, was determined from the reflectance and transmittance of the film as described previously [24,26].

Received: September 18, 1996
Final version: December 4, 1996

[1] M. J. Kelly, *Low-Dimensional Semiconductors*, Oxford University Press, Oxford **1995**.
[2] Z. H. Lu, D. J. Lockwood, J.-M. Baribeau, *Nature* **1995**, *378*, 258.
[3] A. P. Alivisatos, *Science* **1996**, *271*, 933.
[4] L. Brus, *Appl. Phys. A* **1991**, *53*, 465.
[5] C. B. Murray, C. R. Kagan, M. G. Bawendi, *Science* **1995**, *270*, 1335.
[6] T. Vossmeyer, L. Katsikas, M. Giersig, I. G. Popovic, K. Diesner, A. Chemseddine, A. Eychmüller, H. Weller, *J. Phys. Chem.* **1994**, *98*, 7665.
[7] E. J. Heller, M. F. Crommie, C. P. Lutz, D. M. Eigler, *Nature* **1994**, *369*, 464.
[8] L. O. Grondahl, *Science* **1926**, *64*, 306.
[9] C. Kittel, *Introduction to Solid State Physics*, 6th ed., Wiley, New York **1986**, Ch. 11.
[10] P. W. Baumeister, *Phys. Rev.* **1961**, *121*, 359.
[11] D. Fröhlich, R. Kenklies, C. Uihlein, C. Schwab, *Phys. Rev. Lett.* **1979**, *43*, 1260.
[12] V. T. Agekyan, *Phys. Status Solidi A* **1977**, *43*, 11.
[13] J. L. Lin, J. P. Wolfe, *Phys. Rev. Lett.* **1993**, *71*, 1222.
[14] A. Mysyrowicz, E. Benson, E. Fortin, *Phys. Rev. Lett.* **1996**, *77*, 896.
[15] D. Snoke, *Science* **1996**, *273*, 1351.
[16] A. Kellersohn, E. Knözinger, W. Langel, M. Giersig, *Adv. Mater.* **1995**, *7*, 652.
[17] C. R. Martin, *Science* **1994**, *266*, 1961.
[18] Y. Golan, L. Margulis, G. Hodes, I. Rubinstein, J. L. Hutchison, *Surf. Sci.* **1994**, *311*, L633.
[19] J. A. Switzer, M. J. Shane, R. J. Phillips, *Science* **1990**, *247*, 444.
[20] J. A. Switzer, T. D. Golden, *Adv. Mater.* **1993**, *5*, 474.
[21] J. A. Switzer, R. P. Raffaelle, R. J. Phillips, C.-J. Hung, T. D. Golden, *Science* **1992**, *258*, 1918.
[22] J. A. Switzer, R. J. Phillips, T. D. Golden, *Appl. Phys. Lett.* **1995**, *66*, 819.
[23] J. A. Switzer, C.-J. Hung, B. E. Breyfogle, M. G. Shumsky, R. Van Leeuwen, T. D. Golden, *Science* **1994**, *264*, 1573.
[24] R. A. Van Leeuwen, C.-J. Hung, D. R. Kammler, J. A. Switzer, *J. Phys. Chem.* **1995**, *99*, 15247.
[25] A. E. Rakhshani, *Solid-State Electron.* **1986**, *29*, 7.
[26] T. D. Golden, M. G. Shumsky, Y. Zhou, R. A. VanderWerf, R. A. Van Leeuwen, J. A. Switzer, *Chem. Mater.* **1996**, *8*, 2499.
[27] B. Rush, J. Newman, *J. Electrochem. Soc.* **1995**, *142*, 3770.
[28] W. Wolf, K. Krischer, M. Lübke, M. Eiswirth, G. Ertl, *J. Electroanal. Chem.* **1995**, *385*, 85.
[29] H. D. Dewald, P. Rarmananda, R. W. Rollins, *J. Electrochem. Soc.* **1993**, *140*, 1969.
[30] R. A. Young, in *The Rietveld Method* (Ed: R. A. Young), Oxford University Press, Oxford **1995**, Ch. 1.
[31] H. P. Klug, L. E. Alexander, *X-Ray Diffraction Procedures for Polycrystalline and Amorphous Materials*, 2nd ed., Wiley, New York **1974**, p. 656.
[32] Y. Kayanuma, *Phys. Rev. B* **1988**, *38*, 9797.

Information about the VCH Materials Science, Chemistry and Physics Programs is available on the World Wide Web at

http://vch.group.de

including the Tables of Contents of journals prior to publication.

© VCH Verlagsgesellschaft mbH, D-69469 Weinheim, 1997
0935-9648/97/0403-0338 $ 10.00+.25/0